

Crystal Transformation Behavior and Structural Changes of the Planar Zigzag Form for Syndiotactic Polypropylene

Yasumasa Ohira and Fumitaka Horii*

Institute for Chemical Research, Kyoto University, Uji, Kyoto 611-0011, Japan

Takahiko Nakaoki

Faculty of Science and Technology, Ryukoku University, Otsu, Shiga 520-2194, Japan

Received February 28, 2000; Revised Manuscript Received May 8, 2000

ABSTRACT: Crystal transformation behavior and structural changes for the planar zigzag form (form III) of syndiotactic polypropylene, which is spontaneously crystallized at 0 °C from the melt, have been investigated in the heating process by DSC, wide-angle X-ray diffractometry, and high-resolution solid-state ^{13}C NMR spectroscopy. The DSC curve for the sample containing only form III crystallites, which is crystallized at 0 °C for 5000 h, shows an evident endothermic peak at about 20 °C and an additional exothermic peak at about 100 °C prior to melting at about 150 °C. The endothermic peak, which is shifted up to about 40 °C by annealing at room temperature, is found to be ascribed to the crystal transformation from form III with the planar zigzag conformation to form II composed of isochiral helices with the *ttgg* conformation by wide-angle X-ray diffractometry. Moreover, the CH_3 resonance lines of the dipolar decoupling/MAS ^{13}C NMR spectra measured at different temperatures for the sample with almost the same structure as for DSC and WAXD measurements are well resolved into the components with the *tt* and *tg* conformations for the $\text{CH}_2\text{--CH}(\text{CH}_3)\text{--CH}_2$ bond. As a result, it is found that about 16% form III is allowed to be transformed into form II, whereas most of form III is melted gradually in the transition temperature region and very rapidly above that temperature. Such melting of form III should induce the crystallization of form I above about 60 °C, and the final degree of crystallinity of form I attains to almost the same level as for the original form III. This process is really reflected on the appearance of the exothermic peak at about 100 °C in the DSC curve described above. An annealing effect of form III crystallites has also been examined just below the crystal transformation temperature from form III to II.

Introduction

In our previous papers,^{1–3} we have found for the first time that the planar zigzag form (form III^{4–11}) for syndiotactic polypropylene (sPP) is spontaneously crystallized at low temperatures around 0 °C from the melt without any drawing procedure. The highest degree of crystallinity of form III is obtained at 0 °C, but it is still of the order of 0.13 even after the crystallization for 4300 h. When the sample is annealed at room temperature, additional crystallization of form III leads to the increase in crystallinity up to about 0.3. However, the crystallization of form I^{4,5,12–19} with the *ttgg* conformation, which is the most stable form of sPP, is completely suppressed even for the sample with such a low crystallinity. Therefore, some different levels of structural changes will be probably induced when the sample is further heated to higher temperatures. Moreover, it has already been reported mainly by high-resolution solid-state ^{13}C NMR spectroscopy^{5,6} that form III is allowed to transform into another crystal form with the *ttgg* conformation at about 50 °C in the heating process. Lotz et al.²⁰ also suggested that form II composed of isochiral helices with the *ttgg* conformation might be preferentially transformed from form III with the planar zigzag conformation because of steric hindrance. However, the actual crystal transformation process from form III spontaneously crystallized to form II has not been examined by appropriate analytical methods as yet.

In this paper, we investigate possible structural changes and the crystal transformation behavior of form III in the heating process in detail by differential

scanning calorimetry, wide-angle X-ray diffraction, and high-resolution solid-state ^{13}C NMR measurements. In particular, the CH_3 resonance lines for the sPP samples crystallized at 0 °C are precisely analyzed in terms of the components with the *tt* and *tg* conformations for the $\text{CH}_2\text{--CH}(\text{CH}_3)\text{--CH}_2$ bond to obtain the information about the change in degree of crystallinity of each crystal form as a function of temperature. The characteristic trans-rich chain conformation in the noncrystalline state, which is allowed to induce the crystallization of form III with the planar zigzag conformation at lower temperatures, will be analyzed by a similar method in another paper.²¹

Experimental Section

Samples. The sPP sample with racemic triad of 0.96, which was provided by Sumitomo Chemical Co. Ltd., was first pressed to a film with a thickness of about 100 μm at 170 °C and quenched into ice–water.² After again melted at 170 °C for 10 min under a N_2 atmosphere in an aluminum foil containing a spacer for the film, this film was then rapidly quenched into ice–water and crystallized at 0 °C for various periods. For measurements at lower temperatures, the samples crystallized at 0 °C were rapidly cooled to the boiling point of N_2 and was cut into squares of several millimeters. The samples thus obtained were quickly set up to each apparatus kept at an appropriate temperature without leaving the sample temperature above 0 °C.

Differential Scanning Calorimetry. Thermal transition behavior for the sPP samples crystallized at 0 °C was measured on a TA Instruments DSC 2910 differential scanning calorimeter calibrated with indium. The measurements were performed in the region of –30 to 170 °C at a heating or cooling rate of 10 °C/min.

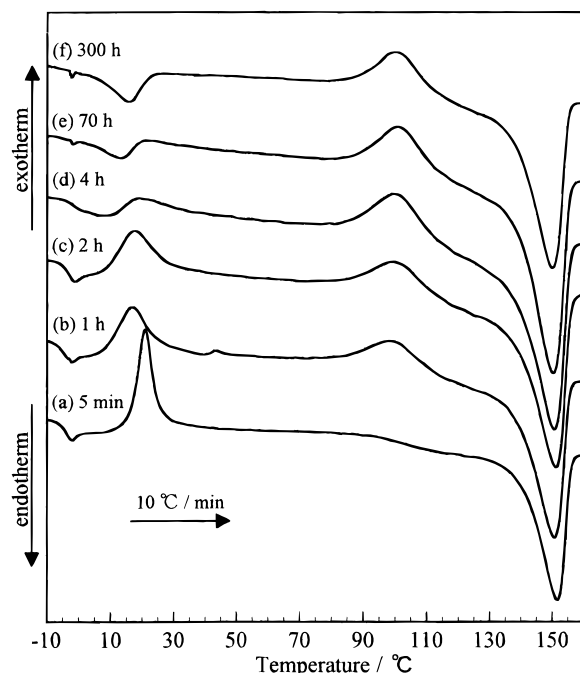


Figure 1. DSC curves measured at a heating rate of 10 °C/min for sPP samples crystallized at 0 °C for different periods from the melt, without heating them up above 0 °C before DSC measurements.

Solid-State ^{13}C NMR Measurements. Solid-state ^{13}C NMR measurements were carried out at 0 °C on a JEOL JNM-GSX200 spectrometer, equipped with a partly modified JEOL variable temperature system, at a static magnetic field of 4.7 T.^{2,22–28} The ^1H and ^{13}C field strengths $\gamma B_1/2\pi$ were 62.5 kHz. Each sample was spun in a zirconia MAS rotor at a speed of 3.0 kHz. Dipolar decoupling (DD)/MAS ^{13}C NMR spectra were collected with transients of 256, using the pulse delay time of 5 s after the acquisition of FID which was 5 times longer than the longest spin–lattice relaxation time $T_{1\rho}$ for the CH_3 carbon. ^{13}C chemical shifts were expressed as values relative to tetramethylsilane (Me_4Si) by using the CH_3 line at 17.36 ppm of hexamethylbenzene crystals as an external reference. The sample temperature was calibrated using the temperature dependence of relative chemical shifts of CH_2 and OH protons of ethylene glycol in a glass ampule^{29–31} which was packed with KBr in the MAS rotor.

Wide-Angle X-ray Diffraction Measurements. Wide-angle X-ray diffraction patterns were obtained with an automatic Rigaku diffractometer equipped with a homemade variable temperature system, using Ni-filtered $\text{Cu K}\alpha$ radiation. The scanning range of 2θ was from 5° to 50° with a step of 0.02° and a scan speed of 2°/min.

Results and Discussion

Figure 1 shows DSC curves measured at a heating rate of 10 °C/min for the sPP samples crystallized at 0 °C for different periods. Each sample was not heated above 0 °C before the DSC measurements. Numerical values at the left side indicate the periods for the crystallization at 0 °C. In the DSC curve for the sample with a very short crystallization time, as shown in Figure 1a, the glass transition of the quenched sPP is evidently observed at about −5 °C, and a prominent exothermic peak additionally appears at about 20 °C prior to melting at about 150 °C. The wide-angle X-ray diffraction pattern measured at 0 °C revealed that this sample is in the noncrystalline state.² Moreover, form I composed of antichiral helices with the *ttgg* conformation was confirmed to be produced for the sample after

annealed above 20 °C by wide-angle X-ray diffractometry. Accordingly, the exothermic peak at about 20 °C should be ascribed to the crystallization of form I.

With increasing crystallization time at 0 °C, however, the exothermic peak due to the crystallization of form I clearly broadens and decreases in intensity. Finally, there seems to be almost no exothermic contribution around 20 °C for the sample crystallized for 300 h as shown in Figure 1f. As already reported in previous papers,^{1–3} form III with the planar zigzag conformation is crystallized at 0 °C during these periods. Therefore, the crystallization of form I at about 20 °C will be suppressed by the crystallization of form III and also by the production of possible aggregates of trans-rich segments in the noncrystalline region at 0 °C, as pointed out in our previous paper.² Moreover, a certain endothermic peak seems to overlap the exothermic contribution, because such an endothermic peak can be clearly observed at about 16 °C for the sample crystallized at 0 °C for 300 h (Figure 1f). This endothermic peak should be assigned to the crystal transformation of form III, as shown in detail somewhat later.

In addition, it is worth noting that another broad exothermic peak appears at about 100 °C for the samples crystallized at 0 °C for longer periods. Such an appearance seems to be related to the suppression of the exothermic peak for the crystallization of form I at about 20 °C. In fact, it is shown later that some rearrangement in the noncrystalline region as a result of partial melting of form III will induce the further crystallization of form I at higher temperatures around 100 °C. It should be also noted here that the glass transition appearing at about −5 °C for the quenched sample becomes gradually difficult to observe for the samples crystallized at 0 °C for longer periods. This fact supports our previous model that some aggregates composed of trans-rich segments may be produced in the noncrystalline region, and the resulting restriction may hinder the crystallization of form I around room temperature.²

As for the crystal transformation of form III, it was reported to occur at about 50 °C for the cold-drawn sPP sample.^{5,6} However, the endothermic peak corresponding to this transformation seems to appear at about 16 °C for the sample crystallized at 0 °C for 300 h as pointed out above (Figure 1f). To clarify the cause of the difference in transformation temperature of form III, we have examined an annealing effect of our sample on the transformation because the crystallinity was found to be much improved by annealing at room temperature.² Figure 2 shows the DSC curve measured at a heating rate of 10 °C/min for the sampled crystallized at 0 °C for 5000 h and then left at room temperature for about 3 months. The first DSC run clearly indicates that the endothermic peak in question shifts to about 44 °C, in good accord with the previous result for the cold-drawn sample.^{5,6} Therefore, the endothermic peak can be assigned to the crystal transformation from form III to another crystal form that will be characterized in detail below. Although such an annealing effect at room temperature is evident, it should be pointed out that the main structural change by the annealing is completed within 1 h for the samples crystallized at 0 °C as revealed by wide-angle X-ray diffractometry and FT-IR spectroscopy.^{2,3}

To make the crystal transformation and partial melting of form III clearer, the second DSC run was carried

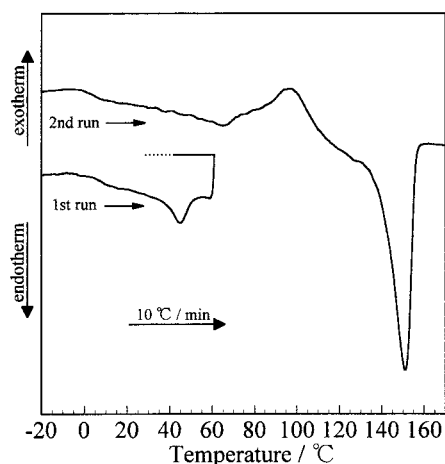


Figure 2. DSC curves at different runs for the sPP sample left at room temperature for about 3 months after crystallized at 0 °C for 5000 h. At the first run the sample was heated to 60 °C and then cooled to −30 °C at a rate of 10 °C/min. After such cooling the second run was started at the same heating rate.

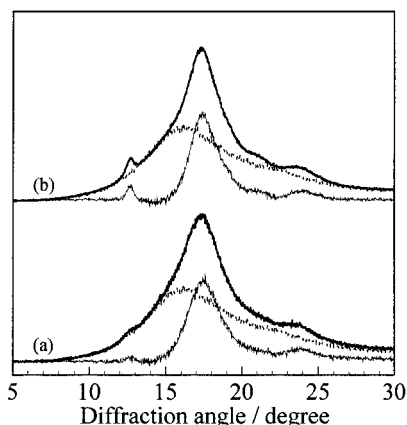


Figure 3. Wide-angle X-ray diffraction profiles for the sPP samples used for the first (a) and the second (b) DSC runs shown in Figure 2.

out for the same sample cooled to −30 °C at a rate of 10 °C/min after the first run up to 60 °C as shown in Figure 2. In contrast to the case of the first run, no endothermic peak corresponding to the crystal transformation appears at the second run, indicating that this transformation is an irreversible process. Instead of the transition peak, a very broad endothermic peak becomes explicitly observable in this temperature region. This broad peak may be ascribed to partial melting of form III which will be quantitatively characterized by solid-state ^{13}C NMR spectroscopy later. However, the further melting endothermic curve for most of form III may disappear probably as a result of the superposition of the exothermic contribution from the crystallization of form I induced in the same temperature region. The less integrated intensity of the exothermic peak around 100 °C compared to that of the melting peak mainly for form I at about 150 °C also suggests such superposition of the melting of form III and the crystallization of form I in this temperature region.

Figure 3 shows wide-angle X-ray diffraction patterns obtained at room temperature for the samples used for the first and second DSC runs shown in Figure 2. The comparison of these diffraction patterns will indicate the structural change induced by the crystal transformation

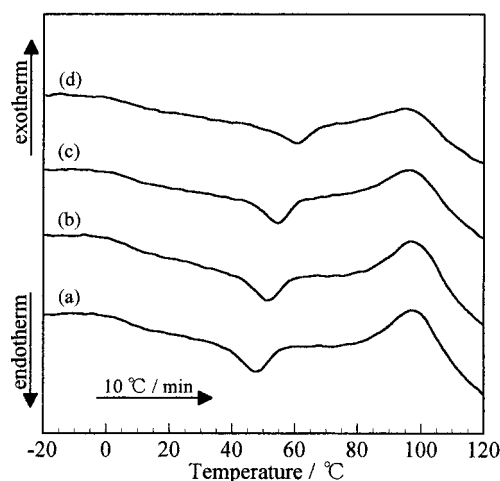


Figure 4. DSC curves for the sPP samples annealed under different conditions. (a), (b), and (c) are for the samples annealed at 32 °C for 0, 90, and 1200 h after crystallized at 0 °C for 5000 h and left at room temperature for about several months, respectively. (d) is for the sample further annealed at 40 °C for 400 h after annealed at 32 °C for 1500 h.

of form III. To make the structural change clear, the total diffraction profiles are resolved into the crystalline and noncrystalline diffraction profiles, which are respectively depicted by thin and dotted curves, by the subtraction method previously reported.² In this case the diffraction profile measured at 0 °C for the amorphous sPP sample just after quenching to 0 °C from the melt was used as an elementary curve for the noncrystalline contribution. In fact, a somewhat sharp reflection peak is observed at $2\theta \sim 12^\circ$ for the sample used for the second DSC run as shown in Figure 3b, although the broad peak assignable to the (020)/(110) planes for form III² still appears there at about 17° . This fact strongly suggests the formation of form I^{14–19} or form II^{7,15,17,19} through the partial crystal transformation of form III, but other reflection peaks at $2\theta \sim 16^\circ$ and 21° closely associated with the discrimination of these crystal forms are not clearly observed in these profiles.

One of the reasons for such a difficulty in characterization may be the low crystallinity for form III. As reported in a previous paper,² the degree of crystallinity of form III was as low as about 0.32 for the sample even after being annealed at room temperature. The crystallite size was found to be also as small as about 7 nm at 0 °C, and no significant increase in size was observed by annealing at room temperature.² To examine the possibility to produce form III samples with much higher crystallinity and to characterize the crystal transformation of form III in more detail, annealing has been performed at temperatures just below the crystal transformation temperature. Figure 4 shows DSC curves for such annealed sPP samples. Figure 4a is the DSC curve for the sample left at room temperature for about several months after being crystallized at 0 °C for 5000 h. Parts b and c of Figure 4 are DSC curves obtained after annealing of this sample at 32 °C for 90 and 1200 h, respectively. With increasing annealing time at 32 °C, the transition peak is found to clearly shift from about 47 to 55 °C. However, the transition enthalpy seems to stay almost constant irrespective of the annealing time, indicating almost no increase in degree of crystallinity of form III. Since no further increase in the transition temperature was observed for the sample annealed at 32 °C for 1500 h, a part of this sample was

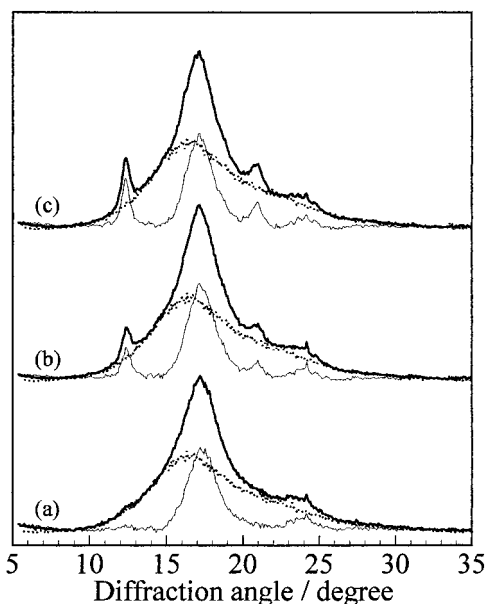


Figure 5. Wide-angle X-ray diffraction profiles for the sPP samples annealed at different conditions. (a), (b), and (c) correspond to (a), (b), and (d) in Figure 4, respectively.

further annealed at 40 °C for 400 h. Figure 4d shows the DSC curve of this sample. The transition temperature is further shifted to about 60 °C, but the integrated peak intensity seems to decrease significantly by annealing at 40 °C. Partial melting and also partial crystal transformation of form III may occur during annealing at 40 °C.

Figure 5 shows wide-angle X-ray diffraction profiles obtained at room temperature for the same samples used for DSC measurements shown in Figure 4. Although the samples shown in Figure 5b,c were subjected to annealing below the transition temperatures for long periods, more enhanced reflection peaks appear at $2\theta = \sim 12^\circ$ and 21° compared to the case shown in Figure 3b. This fact indicates that some amount of form III will be transformed during such annealing, and the crystallinity of the crystallites thus produced may be increased through the long-term annealing. The significant reduction in transition enthalpy observed in Figure 4d will be in good accord with the possible crystal transformation below the transition temperature. Now the assignment of the crystal form produced seems to more readily made compared to the case shown in Figure 3b. The reflections at $2\theta = \sim 12^\circ$ and 21° are ascribed to both form I and form II, but there is no reflection peak at $2\theta = \sim 16^\circ$ that is normally observed for form I.^{14–19} It is, therefore, concluded that form II is preferentially produced through the crystal transformation from form III. In fact, no reflection peak also appears at $2\theta = \sim 16^\circ$ for the sample that really underwent the crystal transformation, as shown in Figure 3b. Long-term annealing must be indispensable for the production of form II with higher crystallinity. The conclusion obtained here will support the mechanism recently proposed for the formation of form II: Form II containing isochiral helices with the *ttgg* conformation should be preferentially transformed from form III with the planar zigzag conformation for steric reasons, although form I composed of antichiral helices with the same *ttgg* conformation is the most stable crystal form of sPP.²⁰

For form III, in contrast to the case of form II, only a very minor decrease in line width, which may cor-

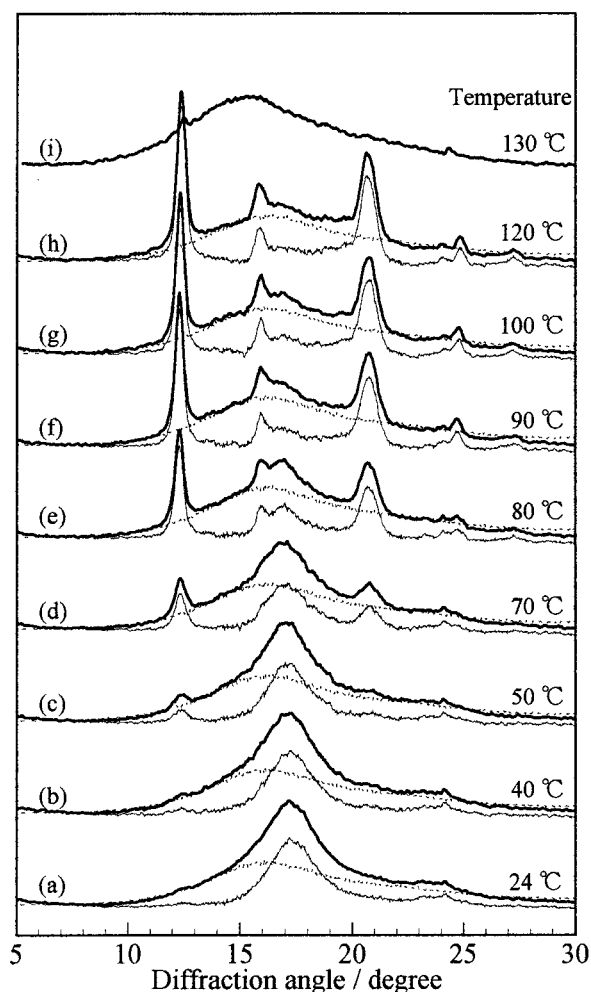


Figure 6. Wide-angle X-ray diffraction profiles measured at different temperatures in the heating process for the sPP sample crystallized at 0 °C for 5000 h.

respond to the increase in transition temperature detected in Figure 2, is observed in Figure 5 for the broad diffraction peak at $2\theta = \sim 17^\circ$ that is assigned to the (020)/(110) planes for form III.¹⁰ Accordingly, it should be noted that the crystallinity of form III involving the crystallite size cannot be greatly improved by long-term annealing at temperatures even just below the transition temperature. The cause for the difficulty may be associated with the chain conformation in the noncrystalline region: The trans-rich conformation at lower temperatures,² which may induce the crystallization of form III, has recently been found to change to the normally trans-gauche distributed conformation in the temperature region of 30–50 °C.²¹ The detailed characterization of the conformation for the noncrystalline segments will be published somewhere in the near future.²¹

To clarify the structural changes as a function of temperature detected by the DSC measurements, wide-angle X-ray diffractometry and high-resolution solid-state ¹³C NMR spectroscopy have been performed in the heating process for the sample crystallized at 0 °C for longer periods. Wide-angle X-ray diffraction profiles measured at different temperatures for the sample crystallized at 0 °C for 5000 h is shown in Figure 6 as thick solid lines. These total diffraction profiles are also resolved into the crystalline and noncrystalline diffraction profiles, which are respectively depicted by thin and

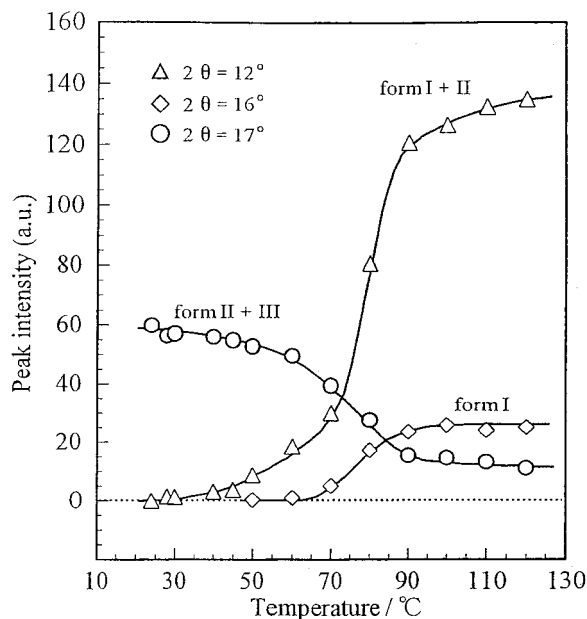


Figure 7. Temperature dependencies of peak intensities for diffraction peaks located at $2\theta = 12^\circ$, 16° , and 17° in the diffraction profiles shown in Figure 6.

dotted curves, by the subtraction method previously reported.² Here it should be noted that the $h20$ reflections are streaked probably due to stacking disorders for forms I and II,¹⁴ and a diffuse reflection produced by this cause in the powder pattern may be partly overlapped on the noncrystalline contribution in Figure 6. However, such a contribution may not significantly affect the separation of the crystalline and noncrystalline profiles, because the apparent degrees of crystallinity obtained by this separation are very close to the values quantitatively determined by solid-state ^{13}C NMR spectroscopy as shown later.

The crystalline profile thus obtained at 24 $^\circ\text{C}$ shows broad but evident reflections around $2\theta = 17^\circ$ and 24° that were respectively assigned to the (020)/(110) and (021)/(111) planes¹⁰ for form III with the planar zigzag conformation, as shown in Figure 6a. With increasing temperature, however, other sharper reflections appear at $2\theta = \sim 12^\circ$, 16° , and 21° above 70 $^\circ\text{C}$. Since these reflections are ascribed to form I composed of antichiral helices with the *ttgg* conformation,^{14–19} this form is found to be crystallized above about 70 $^\circ\text{C}$. It is, therefore, confirmed that the appearance of the exothermic peak in the corresponding temperature region on the DSC curves shown in Figures 1 and 4 is due to the crystallization of form I.

In contrast, it seems again somewhat difficult to observe reflections ascribed to form II at 40 and 50 $^\circ\text{C}$. However, since a broad reflection assignable to form II appears at about $2\theta = \sim 12^\circ$ and no reflection ascribed to form I is observed at $2\theta = \sim 16^\circ$, it is confirmed that form II is produced around 40 $^\circ\text{C}$ as a result of the partial crystal transformation of form III.

In Figure 7 is plotted the peak intensities of the reflections at $2\theta = \sim 12^\circ$, 16° , and 17° shown in Figure 6 against the temperature. Here, the reflection at about 16° is simply due to form I, whereas the reflections at about 12° and 17° contain the contributions from form I/form II and form II/form III, respectively. It is clearly confirmed, in good accord with the DSC results, that form I is crystallized above about 60 $^\circ\text{C}$, and form II is

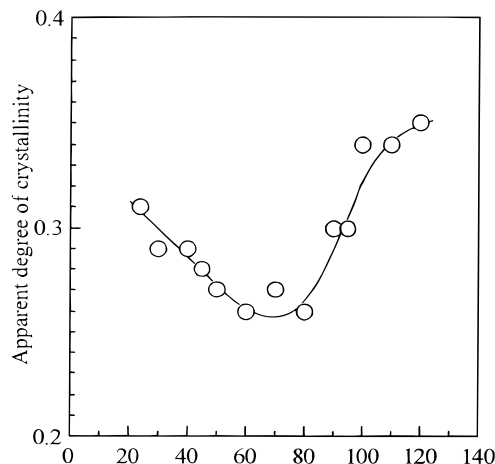


Figure 8. Apparent overall degree of crystallinity for various crystal forms as a function of temperature, obtained from the wide-angle X-ray diffraction profiles shown in Figure 6.

produced with the reduction in form III as a result of the crystal transformation. However, the quantitative changes in their degrees of crystallinity cannot be obtained from this figure. Such detailed information will be given later by high-resolution solid-state ^{13}C NMR spectroscopy. Nevertheless, it should be noted here that the peak intensity at 17° is rapidly changed in the temperature region of 60–90 $^\circ\text{C}$. To examine the possibility of partial melting in this temperature region for the cause, the apparent overall degree of crystallinity has been obtained as $1 - x_a$. Here x_a is an intensity factor for the noncrystalline contribution used for the subtraction of this contribution from the total profile shown in Figure 6 as described in a previous paper.²

The temperature dependence of the apparent overall degree of crystallinity thus obtained is shown in Figure 8. With the increase of the temperature from room temperature to about 70 $^\circ\text{C}$, the apparent degree of crystallinity is evidently decreased from 0.31 to 0.27. Although a part of form III is transformed into form II in this temperature region, this decrease is due to partial melting of form III crystallites as indicated more directly by the high-resolution solid-state ^{13}C NMR analysis later. Above 70 $^\circ\text{C}$, the apparent degree of crystallinity increases again and reaches to about 0.35 at 120 $^\circ\text{C}$. This increase is ascribed to the crystallization of form I possibly as a result of partial melting of form III crystallites.

Figure 9 shows DD/MAS ^{13}C NMR spectra measured at different temperatures for the sPP sample left at room temperature for several days after crystallized at 0 $^\circ\text{C}$ for 144 h. As described in a previous paper,² the degree of crystallinity of form III is not significantly changed by the longer-term crystallization than 20 h. Therefore, the structure of this sample may be almost the same as that used for the DSC and wide-angle X-ray diffraction measurements described above. For simplicity, only the CH and CH_3 resonance lines are shown in this figure. Since the pulse delay time for the $\pi/2$ single pulse sequence was set to a value (5 s) longer than $5T_{1\rho}$ for the CH_3 carbons, the CH_3 resonance lines reflect their equilibrium magnetizations at the respective temperatures. It is found that these resonance lines can be well resolved into five Lorentzian curves, which are indicated as thin lines, by the computer-aided least-squares method. As for the CH_3 resonance lines, two Lorentzian curves are assumed as contributions from

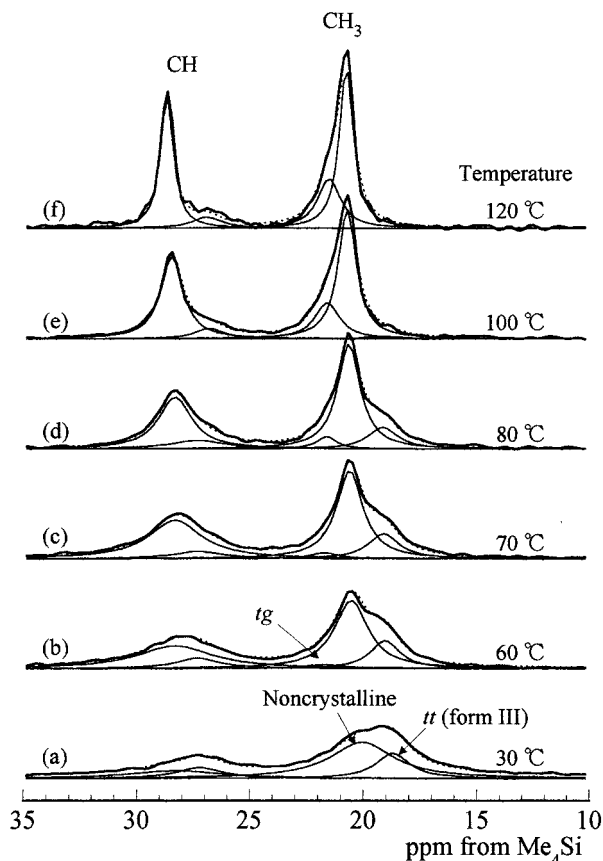


Figure 9. DD/MAS ^{13}C NMR spectra measured at different temperatures in the heating process for the sPP sample crystallized at 0 °C for 144 h.

the crystalline (form III) and noncrystalline components at 30 °C. Here, the form III line is located at the chemical shift corresponding to the *tt* conformation for the $\text{CH}_2\text{--CH}(\text{CH}_3)\text{--CH}_2$ bond, which was defined in a previous paper in detail.² In contrast, the noncrystalline line appears at about 20 ppm as a result of the rapid exchange between the *tt* and *tg* conformations for that bond, whose corresponding resonance lines separately appear at about 19 and 22 ppm at 0 °C, respectively.² It is found that the total CH_3 line is satisfactorily resolved into these two contributions at 30 °C, because the composite curve composed of the two contributions (dotted line) is in good accord with the observed curve.

In contrast, another Lorentzian line should be introduced at 21.6 ppm above 60 °C, and the intensity rapidly increased with increasing temperature. Since the chemical shift of this line corresponds to the CH_3 carbon with the *tg* conformation,² this line can be assigned to the crystalline components of form I and form II. Therefore, the mass fractions of form I and form II are increased above 60 °C with increasing temperature, whereas the fraction of form III is significantly reduced. The noncrystalline line becomes much narrower with the increase of temperature, and the chemical shift seems to concomitantly shift downfield by about 0.6 ppm. The latter phenomenon suggests the increase in gauche fraction for the noncrystalline segments of sPP at higher temperatures. More detailed characterization of the conformation for the noncrystalline component will be made somewhere in the near future.²¹

In contrast to the case of the CH_3 resonance line, the CH line seems to be resolved into two contributions: the crystalline and noncrystalline components that appear

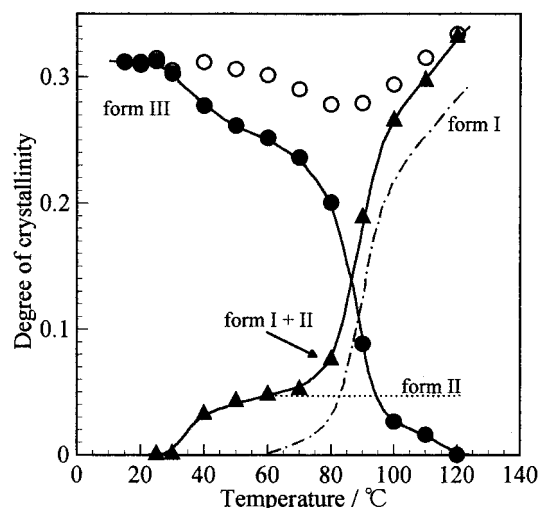


Figure 10. Temperature dependencies of the degrees of crystallinity for the respective crystal forms, obtained by the line shape analysis shown in Figure 9.

upfield and downfield, respectively. Here, the crystalline line is greatly suppressed in intensity because of the longer $T_{1\rho}$ value. Since almost the same extent of the γ -gauche effect may appear for the CH carbons associated with the corresponding trans and gauche conformations, the difference in crystal form cannot be detected for the CH line of sPP. In addition, the CH_2 resonance line also contains information about the structure and structural change for sPP samples. However, the line is considerably broad as shown in Figure 3 in a previous paper,² and it seems therefore difficult to analyze the CH_2 line in detail unlike the case of the CH_3 line.

In Figure 10 the degrees of crystallinity of different crystal forms, which are obtained as integrated fractions of the corresponding CH_3 resonance lines shown in Figure 9, are plotted against the temperature. Here, the overall degree x_c of crystallinity is also shown at each temperature by an open circle. The temperature dependence of x_c , which seems to be in good accord with the result shown in Figure 8, is now well interpreted in terms of the changes in degrees of crystallinity of the respective crystal forms. First, it is clearly found that form III begins to decrease in the degree of crystallinity above about 30 °C. In contrast to this decrease, the total degree of crystallinity of forms I and II increases rapidly above about 30 °C. Since form I is crystallized above 60 °C as observed in Figure 7, this increase is found to be due to the production of form II through the partial crystal transformation from form III. Moreover, the transformation is completed below 60 °C as observed by the DSC thermogram shown in Figure 2. By considering these experimental facts, it is concluded that the change in degree of crystallinity for form II should be described as a dotted line indicated by form II in Figure 10. As a result, a chain line for form I can be also obtained by the subtraction of the contribution of form II from the total degree of crystallinity of forms I and II.

As is clearly seen in Figure 10, the overall degree of crystallinity somewhat decreases below about 85 °C with increasing temperature. This fact indicates that a small amount of form III (about 0.02 as absolute fraction) is melted below 60 °C during the crystal transformation into form II. Such melting will relax the restriction in the noncrystalline region and finally

induce the crystallization of form I that is the most stable crystal form of sPP. Moreover, most of form III is rapidly melted above 60 °C, and the resulting crystallization of form I is markedly induced. In contrast, only about 16% form III is found to be transformed into form II at 30–60 °C, because the final degree of crystallinity of form II is about 0.05 as seen in Figure 10.

Finally, we briefly discuss about the possible cause of the existence of two types of form III crystallites, ones being transformed to form II and others being melted without the association with the crystal transformation. As already described, the crystallinity of form III is considerably low. Although the cause of such low crystallinity is not clear at present, the crystallites should also contain some amount of defects which may be mainly introduced by the longitudinal disordering of the planar zigzag chains along the chain axis. If the local concentration of such defects would be relatively high, the crystal transformation could be induced to produce form II composed of the isochiral helices with the *ttgg* conformation. Some local environmental condition should be fulfilled by the existence of the defects to induce the crystal transformation to form II. In contrast, most of form III crystallites with less defects may be simply melted without the association with the crystal transformation. However, it would be very difficult to confirm the existence of two types of form III crystallites by analytical methods. Further longer-term annealing below the transition temperature may give a clue to understanding the mechanism of the production and the growth of the form II crystallites. As for form I composed of antichiral helices with the same *ttgg* conformation, the crystallization seems to occur from isotropic random chains or at least in the noncrystalline state even if the chains have trans-rich conformations at lower temperatures.²¹ More detailed discussion about the crystallization process of different crystal forms of sPP will be made somewhere in the future.

Conclusion

Crystal transformation behavior and the structural changes of form III for sPP have been investigated in the heating process by DSC, wide-angle X-ray diffraction, and high-resolution solid-state ¹³C NMR measurements, and the following conclusions have been obtained:

(1) In DSC curves for sPP samples crystallized at 0 °C for shorter periods, one exothermic peak assignable to the crystallization of form I appears at about 20 °C prior to melting in the heating process when the samples are not heated above 0 °C before DSC measurements. In contrast, a somewhat broad endothermic peak appears at about 15 °C, and the exothermic peak is shifted up to about 100 °C for the samples crystallized at 0 °C for longer periods.

(2) When the sample crystallized at 0 °C for 5000 h is annealed at room temperature, the endothermic peak described above is shifted to about 40 °C, which is in good accord with the temperature for the crystal transformation from form III to II previously reported. In fact, the analysis of wide-angle X-ray diffraction profiles measured for samples annealed at different temperatures below the crystal transformation temperatures clearly indicates the production of form II through the partial crystal transformation of form III. Therefore, this fact will support the previous proposal that form II containing isochiral helices with the *ttgg* conformation

is preferentially transformed from form III with the planar zigzag conformation owing to the steric hindrance although form I composed of the antichiral helices is thermodynamically the most stable crystal form of sPP.

(3) The CH₃ resonance lines of DD/MAS ¹³C NMR spectra measured at different temperatures for the sPP sample, which has almost the same structure as for the DSC and WAXD measurements, are precisely analyzed in terms of the components with the *tt* and *tg* conformations for the CH₂–CH(CH₃)–CH₂ bond. As a result, about 16% form III is found to be really transformed into form II, whereas about 84% residual form III is melted in the temperature region of 30–120 °C. Moreover, it is confirmed, in good accord with the appearance of the exothermic peak on the DSC curve described above, that form I is crystallized above 60 °C as a result of the melting of form III although this crystallization is completely suppressed at lower temperatures for the samples crystallized at 0 °C for longer periods.

(4) To improve the crystallinity of form III, annealing of the sPP sample crystallized at 0 °C for a long period is carried out just below the crystal transformation temperature. However, the degree of crystallinity of form III is significantly decreased by the partial transformation into form II during annealing although the transformation temperature is clearly increased from about 47 to 60 °C.

Acknowledgment. We thanks Drs. Hitoshi Miura and Hiroaki Katayama of Sumitomo Chemical Co. Ltd. for providing the highly syndiotactic polypropylene sample.

References and Notes

- (1) Nakaoki, T.; Ohira, Y.; Hayashi, H.; Horii, F. *Macromolecules* **1998**, *31*, 2705.
- (2) Ohira, Y.; Horii, F.; Nakaoki, T. *Macromolecules* **2000**, *33*, 1801.
- (3) Nakaoki, T.; Yamanaka, T.; Ohira, Y.; Horii, F. *Macromolecules* **2000**, *33*, 2718.
- (4) Tadokoro, H.; Kobayashi, M.; Kobayashi, S.; Yasufuku, K.; Mori, K. *Rep. Prog. Polym. Phys. Jpn.* **1966**, *9*, 181.
- (5) Sozzani, P.; Simonutti, R.; Comotti, A. *Magn. Reson. Chem.* **1994**, *32*, s45.
- (6) Asakura, T.; Aoki, A.; Date, T.; Demura, M.; Asanuma, T. *Polym. J.* **1996**, *28*, 24.
- (7) De Rosa, C.; Auriemma, F.; Vinti, V. *Macromolecules* **1998**, *31*, 7430.
- (8) Natta, G.; Corradini, P.; Ganis, P. *Makromol. Chem.* **1960**, *39*, 238.
- (9) Natta, G.; Peraldo, M.; Allegra, G. *Makromol. Chem.* **1964**, *75*, 215.
- (10) Chatani, Y.; Maruyama, H.; Noguchi, K.; Asanuma, T.; Shiomura, T. *J. Polym. Sci., Polym. Phys. Lett.* **1990**, *28*, 393.
- (11) Sozzani, P.; Galimberti, M.; Balbontin, G. *Makromol. Chem., Rapid Commun.* **1992**, *13*, 305.
- (12) Corradini, P.; Natta, G.; Ganis, P.; Temussi, P. A. *J. Polym. Sci., Part C* **1967**, *16*, 2477.
- (13) Lovinger, A. J.; Davis, D. D.; Lotz, B. *Macromolecules* **1991**, *24*, 552.
- (14) Lovinger, A. J.; Lotz, B.; Padden, F. J. *Macromolecules* **1993**, *26*, 3494.
- (15) De Rosa, C.; Corradini, P. *Macromolecules* **1993**, *26*, 5711.
- (16) De Rosa, C.; Auriemma, F.; Corradini, P. *Macromolecules* **1996**, *29*, 7452.
- (17) Auriemma, F.; Lewis, R. H.; Spiess, H. W.; De Rosa, C. *Macromol. Chem. Phys.* **1995**, *196*, 4011.
- (18) De Rosa, C.; Auriemma, F.; Vinti, V. *Macromolecules* **1997**, *30*, 4137.
- (19) Auriemma, F.; De Rosa, C.; Ruiz de Ballesteros, O.; Corradini, P. *Macromolecules* **1997**, *30*, 6586.

- (20) Lotz, B.; Mathieu, C.; Thierry, A.; Lovinger, A. J.; De Rosa, C.; Ruiz de Ballesteros, O.; Auriemma, F. *Macromolecules* **1998**, *31*, 9253.
- (21) Ohira, Y.; Horii, F.; Nakaoki, T. *Polym. Prepr., Jpn.* **2000**, *49*, 417.
- (22) Kuwabara, K.; Kaji, H.; Horii, F.; Bassett, D. C.; Olley, R. H. *Macromolecules* **1997**, *30*, 7516.
- (23) Kuwabara, K.; Horii, F. *Macromolecules* **1999**, *32*, 5600.
- (24) Masuda, K.; Horii, F. *Macromolecules* **1998**, *31*, 5810.
- (25) Ishida, H.; Kaji, H.; Horii, F. *Macromolecules* **1997**, *30*, 5799.
- (26) Ishida, H.; Horii, F. *Polymer* **1999**, *40*, 3781.
- (27) Yamamoto, H.; Horii, F. *Macromolecules* **1993**, *26*, 1313.
- (28) Yamamoto, H.; Horii, F.; Hirai, A. *Cellulose* **1996**, *3*, 229.
- (29) Kaplan, M. L.; Bovey, F. A.; Chang, H. V. *Anal. Chem.* **1975**, *47*, 1703.
- (30) English, A. D. *J. Magn. Reson.* **1984**, *57*, 491.
- (31) Murata, T.; Horii, F.; Fujito, T. *Proc. Soc. Solid-State NMR Polym.* **1990**, *7*, 29.

MA000357N